IMEKO International Conference on
Metrology for Archaeology and Cultural Heritage
Lecce, Italy, October 23-25, 2017

ToF-SIMS and μ-Raman measurements on laser cleaned bronze archaeological artefacts

Elisabetta Di Francia[1], Ruth Lahoz[2], Delphine Neff[3], Emma Angelini[1], Sabrina Grassini[1]

[1]*Dipartimento di Scienza Applicata e Tecnologia, Politecnico di Torino, Italy*
elisabetta.difrancia@polito.it, emma.angelini@polito.it, sabrina.grassini@polito.it
[2]*Centro de Química y Materiales de Aragón, (CSIC – Universidad de Zaragoza), Zaragoza, Spain, rlahoz@unizar.es*
[3]*NIMBE/LAPA-IRAMAT, CEA/CNRS/U Paris-Saclay, France, delphine.neff@cea.fr*

***Abstract* – In this study, ToF-SIMS and μ-Raman analyses have been employed to assess the feasibility of laser treatments as a selective, non invasive cleaning methodology for archaeological metallic artefacts. A Q-switched Yb:YAG fibre laser, operating at 1064 nm, has been used for the cleaning treatments, carried out in air and ^{18}O rich atmosphere on an ancient bronze coin. The preliminary results show that laser cleaning treatment selectively removes the dangerous oxyhydroxy chlorides corrosion products without affecting the cuprite protective patina grown directly in contact with the metallic surface.**

I. INTRODUCTION

In the restoration field, cleaning is an important and critical phase. As a matter of facts, the amount of material to be removed is a critical and controversial point and the decision is usually based only on the experience of the restorer, becoming very subjective.

On the other hand, it should be taken into account that the corrosion product layers formed on Cu-based archaeological artefacts are characterized by very complex micro-chemical and stratified structures [1,2]. The corrosion product layer is commonly composed by a thin cuprite (Cu_2O) film grown directly on the metallic surface, and by different layers of copper oxides and copper oxyhydroxy chlorides and by other compounds formed by the interaction with the soil. Cuprite commonly acts as a protective layer, which prevents the interaction of reactive copper chloride (CuCl) with oxygen and humidity, thus avoiding the cyclic copper corrosion process, generally called *bronze disease* [3,4]. Therefore, particular attention must be paid during the removal of surface encrustations and corrosion products from bronze artefacts in order to avoid exposing CuCl to air.

In the last years several low invasive cleaning procedures have been investigated in the literature [5,6,7,8,9] for optimising and standardising low invasive and really effective cleaning procedures.

With respect to chemical and mechanical methods, laser cleaning presents several advantages, such as higher accuracy and higher selectivity at micro-scale level. However, notwithstanding the evolution of laser systems allows an increased control on the process, setting the laser parameters as a function of the chemical composition of the corrosion products layer is still a critical action.

In this contest, it is still necessary to increase the understanding of how the laser treatment affects the metallic material in order to optimise the cleaning methodology and assess its real feasibility as a standard conservation procedure for metallic works of art. As a matter of facts, in order to meet all the conservation requirements highlighted by archaeologists and museum curators, it is necessary to optimise high selective, reproducible and non-destructive laser cleaning treatments.

In this study dark-field microscopy, μ-Raman spectroscopy and ToF-SIMS analyses were performed on a bronze coin before and after laser cleaning, to better understand the etching mechanism and how the laser affects the chemical composition of the cleaned surface. Eventually, the efficiency of the laser treatment in removing the dangerous corrosion products without damaging the metallic surface was also assessed.

II. MATERIALS AND METHODS

An ancient bronze Roman Empire coin (Fig.1) was submitted to laser cleaning and after that the metallic surface was characterised from the chemical and morphological point of view. The coin (5.85 g in mass and 24x25 mm in size), was cut in nine samples and the corrosion products were characterised by dark-field microscopy and μ-Raman spectroscopy before and after laser cleaning.

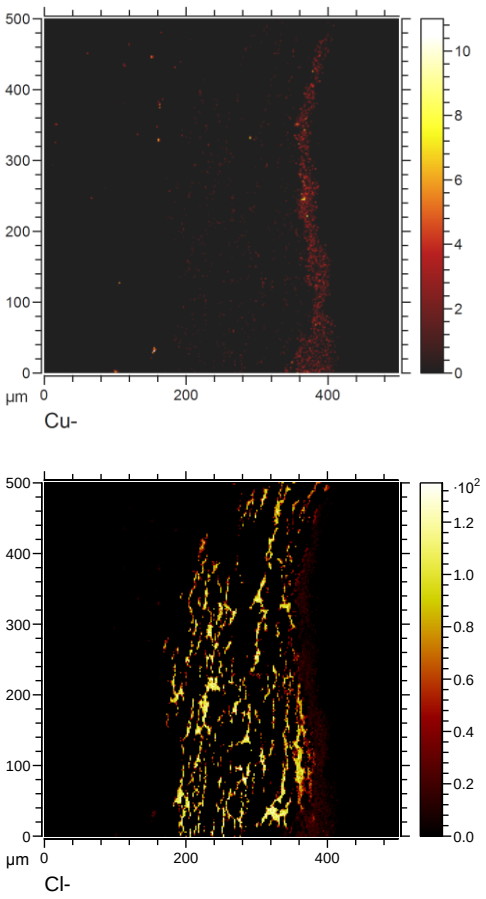

Fig. 5. ToF-SIMS maps of the laser cleaned coin: Cu component (up) and Cl component (down).

IV. CONCLUSIONS

This study evidences the contribution of high advanced analytical techniques in the study of laser-material interation during cleaning treatments performed on archaeological bronze artefacts. Understanding the laser ablation mechanism is the starting point to develop safe and effective laser cleaning treatments.

µ-Raman and ToF-SIMS are important tools for the charaterisation of the corrosion product layer and to investigate the effect of the laser on the corrosion product layer from the chemical point of view. In particular, ToF-SIMS measurments allow to investigate the laser ablation mechanism at the microscale level and to understand if any surface modification occurs by the interaction between the corrosion products and the laser beam.

The preliminary results show that no interaction between the cuprite layer in contact with the metal and the atmosphere occurs during the laser ablation. However, further investigations are ongoing to confirm the preliminary experimental findings here discussed.

V. ACKNOWLEDGEMENTS

The Authors would like to thank the European Federation of Corrosion (EFC) for the support for the measurement campaign in the frame of the EUROCORR Young Scientist Award 2016. A special thank to Jacopo Corsi for the bronze coin donation and to Nicolas Nuns, Université Lille1 (France) for the ToF-SIMS analyses and for his contribution to the discussion of the experimental findings.

VI. REFERENCES

[1] L.Robbiola, J.-M. Blengino, C. Fiaud, "Morphology and mechanisms of formation of natural patinas on archaeological Cu–Sn alloys", on Corrosion Science, vol. 40:12, 1998, p. 2083–2111.

[2] I.Constantinides, A.Adriaens, F.Adams, "Surface characterization of artificial corrosion layers on copper alloy reference materials" on Applied Surface Science, vol.189:1–2, 2002, pp.90–101.

[3] K.Marušić, H. Otmačić-Ćurković, Š. Horvat-Kurbegović, H. Takenouti, E. Stupnišek-Lisac, "Comparative studies of chemical and electrochemical preparation of artificial bronze patinas and their protection by corrosion inhibitor" on Electrochimica Acta, vol.54:27, 2009, p. 7106

[4] T.Kosec, H. Otmačić Ćurković, A. Legat, "Investigation of the corrosion protection of chemically and electrochemically formed patinas on recent bronze", on Electrochimica Acta, vol.56:2, 2010, p. 722.

[5] R.Pini, S.Siano, R.Salimbeni, M.Pasquinucci, M.Miccio, "Tests of laser cleaning on archeological metal artefacts", on Journal of Cultural Heritage, vol.1, 2000, pp. S129–S137.

[6] H.Lee, N. Cho, J. Lee, "Study on surface properties of gilt-bronze artifacts, after Nd:YAG laser cleaning", on Applied Surface Science, vol.284, 2013, pp. 235-241.

[7] E.Di Francia, R. Lahoz, E. Angelini, S. Grassini, M. Parvis, "Pulsed laser cleaning of metallic heritage" on Proc. of 2nd International Conference on Metrology for Archaeology, Torino, Italy, 2016, pp. 77-82.

[8] C. Fenic, R. Dabu, A. Stratan, C. Blanaru, C. Ungureanu, C. Luculescu, "Preliminary studies of material surface cleaning with a multi-pulse passively Q-switched Nd:YAG laser", on Optics & Laser Technology, vol.36:2, 2004, p. 125.

[9] M.Matteini, C. Lalli, I. Tosini, A. Giusti, S. Siano, "Laser and chemical cleaning tests for the conservation of the Porta del Paradiso by Lorenzo Ghiberti", on Journal of Cultural Heritage, vol.4:1, 2003, p. 147.

acquire an image over a 500x500 μm^2 area (512x512 pixels); (3) acquire an image over a 100x100 μm^2 with 512x512 pixels for a more precise observation.

III. RESULTS AND DISCUSSION

As an example, Fig. 3 shows dark-field microscope images of the coin cross section before and after the laser cleaning performed in ^{18}O rich atmosphere. Before the laser treatment the complex corrosion products microstructure can be observed. After the cleaning, the thickness of the corrosion products layer was significatly reduced. However, two main corrosion products layers were still present on the metallic surface; an external compact layer (up to 80 µm) and a 120 µm thick layer in contact with the metallic substrate. It was possible to associate the red and green colour of the corrosion products to the presence of Cu^{+} and Cu^{++} compounds, respectively. From the images it was also possible to see the presence of corrosion compounds interconnected with the bulk of the bronze coin.

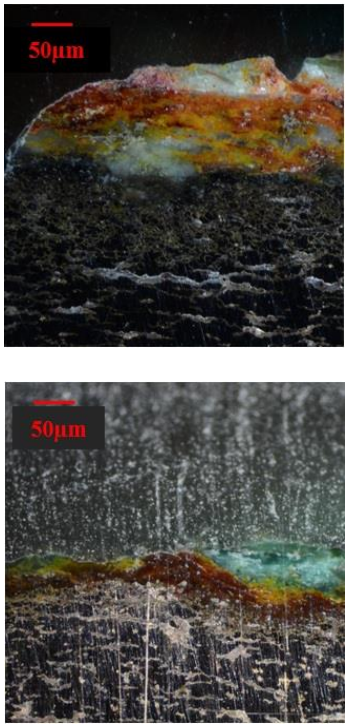

Fig. 3. Dark-field images of the corrosion products layer before (up) and after (down) laser cleaning.

µ-Raman spectra, shown in Fig. 4, confirmed the presence of cuprite (Cu_2O) and clinoatacamite ($Cu_2Cl(OH)_3$) in the corrosion product layer still present on the metal surface after the laser cleaning.

In particular, the presence of a cuprite layer in contact with the metal was evidenced, while the laser ablation succeded in removing most of the oxyhydroxy chlorides corrosion products.

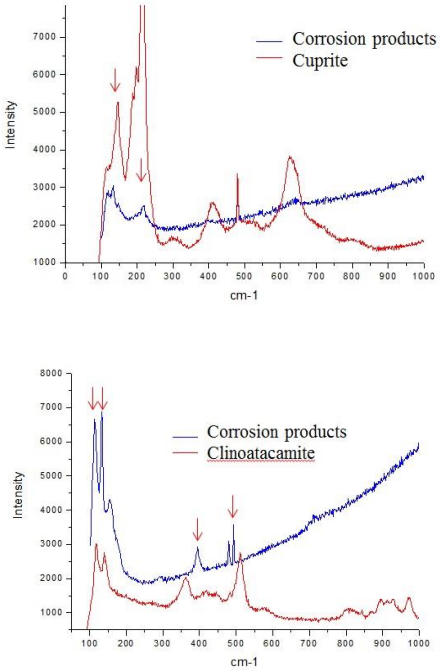

Fig. 4. µ-Raman spectra of the laser cleaned sample and corresponding reference spectra (acquired from powder): identification of cuprite (up) and clinoatacamite (down).

Fig. 5 shows the ToF-SIMS maps of the same sample. The images confirm the morphology, the chemical composition and the thickness of the corrosion products layer: after the laser cleaning treatment, a compact layer of Cu-based compounds was present in contact with the bulk. Then, from the ToF-SIMS map it was also possible to identify the presence of chloride corrosion compounds interconnected with the bulk of the coin. On the contrary, a low concentration of chlorides was detected on the external surface, confirming that most of the oxyhydroxy chlorides were removed during the laser ablation.

The quantitative ToF-SIMS analysis of the oxygen isotopes shows a ratio $^{18}O/(^{16}O+^{18}O)$ around 0.21% in the corrosion product layer, which is approximately the ratio of the two isotopes in the natural air. This value seems to highlight that no interaction occurs between the corrosion product layer and the atmosphere during the laser ablation. However, other analyses are in progress to confirm these preliminary experimental findings.

Fig. 1. Roman Empire coin: recto (right) and verso (left). The images were taken by using a high-resolution digital camera (4000×3000 pixels, Panasonic Lumix G2) and a camera stand equipped with a 4000 K lamp.

To characterise the corrosion products by dark-field microscopy and μ-Raman spectroscopy, the coin cross sections were prepared embedding the samples in SpeciFix-20 (Struers resin) and polishing them with 500 to 4000 SiC paper and with 6 to 1 μm cloths. Dark-field images were acquired with an Olympus BX51 microscope equipped with a Nikon EOS camera.

Due to the not homogeneus thikness of the corrosion product layer on the archaeological artefact, several measures of the thikness layer were done before and after the laser cleaning treatment on the embedded samples on the optical microscopical images.

μ-Raman analyses were performed under a Leica x50/0.85 microscope objective and the spectra were acquired with a Renishaw Invia equipped with a double Nd: YAG laser (532 nm). For the μ-Raman analyses the laser power on the sample surface was fixed to about 500 μW in order to avoid the thermal transformation of the analysed phases.

Pulsed laser cleaning treatment were performed, with the experimental parameters reported in Table 1, with a Q-switch Yb:YAG fibre laser (model EasyMark-20, Jeanologia), operating in the near-IR (1064 nm).

Tab. 1. Laser parameters employed for the laser cleaning treatment on the coin.

Laser Parameters	
Power, *P[W]*	0.73
Fluence, *F [J/cm^2]*	5.16
Irradiance, *I [MW/cm^2]*	1290.94
Pulse duration, t_p *[ns]*	4
Scan speed, v_{scan} *[mm/s]*	300
Repetition rate, f_{rep} *[kHz]*	20
Interlining, *I [μm]*	15

The laser was equipped with a set of galvanometric mirrors to deflect the beam and scan the surface of the sample through a CAD environment software. This software manages the beam movement, allowing different results to be obtained in the surface modification of the material. This set-up allows, besides the control of laser energetic parameters, the acurate use of geometrical overlapping of the laser spots on the surface as another relevant control parameter. The laser treatments were performed both in air and in ^{18}O rich atmosphere to investigate the interaction among the corrosion products, the metallic surface and the atmosphere induced by the laser.

The laser-material interaction, as shown in Fig. 2, is very complex and it is mainly affected by the experimental parameters employed during the treatment. When the laser energy is absorbed by the corrosion products and reflected by the metal, it is possible to optimise a self-limiting and non invasive cleaning treatment. In this condition the laser is effective in removing the corrosion products without damaging the metallic surface.

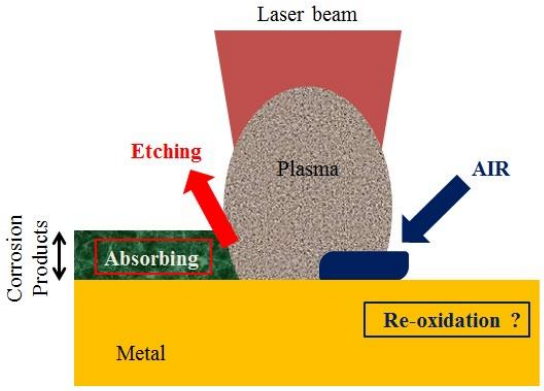

Fig. 2 Laser-material interactions.

However, since the laser treatment is carried out in air, the laser could induce a further re-oxidation of the metallic surface, leading to the formation of a cuprite layer, which is not the cuprite layer originally present on the artefact. Other chemical transformations could occur as well.

In this study, thanks to the presence of ^{18}O isotope in the atmosphere during the laser cleaning treatment, it is possible to understand if any surface re-oxidation occurs during the laser ablation of the corrosion products.

In order to detect the presence of ^{18}O in the corrosion product layer, the coin cross sections were analysed by a ToF-SIMS[5] instrument from IONTOF equipped with bismuth source. A Bi^+ source (0.24 pA, 25kV) was used as primary ions in burst mode (6 pulses). Burst mode provides better lateral resolution and avoids saturation of ^{16}O. The protocol adopted was: (1) etching the surface with Cs^+ sputter gun (2kV, 85nA) rastered over a 800x800 μm^2 to remove organic contamination; (2)